

Spatial Optimization Layout of Best Management Practices through SWAT and Interval Fractional Programming Under Uncertainty

Jinjin Gu (✉ gujinjin@hfut.edu.cn)

Hefei University of Technology

Yuan Cao

College of Architecture and Art, Hefei University of Technology

Min Wu

College of Architecture and Art, Hefei University of Technology

Min Song

College of Architecture and Art, Hefei University of Technology

Lin Wang

College of Architecture and Art, Hefei University of Technology

Research Article

Keywords: Best management practices, Interval fractional programming, Uncertainty, Spatial optimization layout

Posted Date: June 7th, 2021

DOI: <https://doi.org/10.21203/rs.3.rs-509238/v1>

License:  This work is licensed under a Creative Commons Attribution 4.0 International License.

[Read Full License](#)

Spatial Optimization Layout of Best Management Practices through SWAT and Interval Fractional Programming under uncertainty

Jinjin Gu^{a,*}, Yuan Cao^b, Min Wu^a, Min Song^a, Lin Wang^a

^aDepartment of Urban and Rural Planning, College of Architecture and Art, Hefei University of Technology, Hefei 230601, China

^bDepartment of Architecture, College of Architecture and Art, Hefei University of Technology, Hefei 230601, China

Abstract

Uncertainty in nature and human society affect pollution control efficiency and the rationality of the scheme of spatial optimization layout of best management practices (BMP) for agricultural non-point-source (NPS) pollution treatment. Based on this idea, the study innovatively develops a mathematical model that integrates soil and water assessment tool (SWAT) model and interval fractional programming. The advantage of the model are the following: (1) ability to process a BMP spatial optimization layout in watershed in uncertain situations, (2) ability to effectively reflect the uncertain factors involved in the scheme without having to set all the variables as uncertain factors, and (3) results are in the form of schemes in upper and lower limit scenarios, thereby reflecting the limit of uncertainty impact on the schemes.

The results of this study can provide decision-makers with a wide range of optional schemes. This study examines how to set up the BMP spatial optimal layout scheme for agricultural non-point-source pollution treatment under the influence of uncertain factors. The proposed method is universal and can be extended to other cases.

Keyword: Best management practices; Interval fractional programming; Uncertainty; Spatial optimization layout

1. Introduction

A spatial optimal layout of best management practices (BMPs) can effectively alleviate non-point source (NPS) pollution in a river basin. However, deep-rooted uncertainties in nature and human society exist in BMPs, such as in cost and pollutant treatment efficiency (Gu et al, 2020). These uncertainties influence the NPS pollution efficiency and cost of the BMP spatial optimal layout. For example, BMP treatment of NPS pollutants involves many factors, such as reaction time, temperature, rainfall, and various vegetation and microbial species. These factors determine that the efficiency and variation in any one of them would cause variations in the treatment effect. Therefore, the removal effect of pollutants in related studies is expressed in the form of floating intervals, which represent the possible scale of the results caused by uncertainties (Gu et al, 2020). For the uncertainty of cost, the economic cost of BMPs is subject to market fluctuations, and the change reflects the character of the market. Thus, the economic cost is also expressed in the form of floating intervals.

Uncertainties would cause the result of the BMP spatial optimization allocation to be unable to achieve the desired purpose by affecting the pollution treatment efficiency of BMPs. Therefore, the uncertainty factor would also affect the rationality of the spatial optimal layout scheme of BMPs. The reference factors, such as treatment efficiency and cost of BMPs in formulating schemes, are generally set as the definite

value. Thus, the change in the value of reference factors possibly affect the rationality of the spatial optimization scheme.

Many studies have been conducted to solve the problem of uncertain factors in the BMP spatial optimization layout, and genetic algorithm (GA) is widely used (Kaini et al, 2012; Wu et al, 2018). The spatial layout method based on the GA can process the uncertainty and obtain definite results, but the following problems occur in related studies with the GA method:

(1) With GAs, all the related variables need to be set as uncertain values, but in practice, not all variables are uncertain numbers. Therefore, the studies using this method have to set all the related variable factors as uncertainty values with mean values.

(2) It is not convenient for the GA to set complex constraint equations. In general, relevant studies use mathematical software, such as Matlab, to build a GA optimization equation. However, the complex constraints are always difficult to set in these software due to the constraints of integrated software packages. In practical terms, complex constraints for variables are encountered in planning inevitably, whereas the related software with the GA method are not highly suitable for the operator and planner.

(3) It is not convenient for GA to set weight values between multi-objective functions while avoiding subjective judgement. Particularly in dealing with the multi-objective problem of maximum objective function and minimum objective function, setting appropriate weight values between maximization and minimization without subjective judgement is difficult.

Therefore, an important task is to develop a method for BMP spatial optimization layout under uncertainty. The method has to process uncertainty and avoid subjective weights in multi-objective optimization, and should be able to address multiple complex constraints.

1.1 NPS pollution control in watersheds

The first step in NPS pollution control in watersheds is to determine the amount of NPS pollution that should be controlled. In farmland areas, NPS pollution is usually due to nitrogen and phosphorus (P) produced by agricultural activities (Wu and Lu, 2019). The release of NPS pollution can be simulated effectively by using hydrological software. Soil and water assessment tool (SWAT) software is an effective NPS pollution analysis tool that considers environmental factors such as regional topography, soil, land use map, and climate. In addition, this software can systematically analyze the land surface process and channel behavior of pollutant loss, and evaluate the efficiency of the pollution control scheme (Feng and Shen, 2021). When the BMP spatial optimization layout is used to control NPS pollution in watersheds, SWAT software can be used to divide the studied watershed into sub-watershed or hydrology response unit (HRU), and the BMP facilities are allocated to each sub-watershed or HRU (Qiu et al, 2019).

1.2 Spatial optimization layout of BMP facilities

During the BMP spatial optimization layout, the problems of pollutant treatment efficiency and total cost should be considered. Fractional planning can be used to solve the conflict between maximum and minimum objectives, and such planning can

effectively avoid the subjective setting for objective function weights (Gu et al, 2018).

In addition, writing of fractional programming in a more open and basic mathematical programming software can easily load diverse and complex constraint equations.

Fractional programming has been used in many fields.

1.3 Uncertainty analysis

In general, uncertain factors can be expressed in mathematical form according to their mathematical properties, and the form of uncertain numbers can be categorized as interval, random, and fuzzy numbers (Guo et al, 2014). Integrating these uncertain numbers into the optimization model make up the uncertainty optimization model. When uncertainty numbers are integrated into fractional programming, the integrated uncertainty fractional model could be in different forms according to the distribution forms of uncertainty (Zhang et al, 2019). To perform uncertainty programming, the confidence distribution interval is first identified according to the distribution form of the uncertainty number, and then taking the upper and lower boundaries of the interval number into the optimization model to solve the problem. Finally, the upper and lower limit values of the programming model are obtained (Li et al, 2019).

At present, although many studies about uncertain BMP spatial optimization layout have been conducted, most of the related studies use GA to perform the optimization, among which the constraints on the parameter variables are relatively simple (Qi et al, 2020; Getahun and Keefer, 2016). Few studies can reflect the complex constraints for variables in practical problems. Besides, most of the related studies obtain the definite scheme results. Although the definite schemes based on GA consider

the uncertainty factors, the results lack the flexibility to deal with these factors, and it would cause decision-makers to lack the right to choose other schemes according to the complex environment.

Based on these insights, the present study proposes a method that integrates SWAT and uncertainty fractional optimization model to process the NPS in watersheds under uncertainty. SWAT software is used to simulate the emission of NPS pollutants in the study area, and the uncertainty fractional optimization model is applied to solve the problems in the BMP spatial optimization layout. The problems include (1) how to process the uncertainties in the equation, (2) how to avoid subjective weight in multiple objective programming, (3) how to tackle multiple constraints, and (4) how to address inelasticity of a single result.

The study results could serve as theoretical supplement for the study of the BMP spatial optimization layout, and provide a reference for relevant decision-makers in creating schemes.

2. Study area

In this study, a small watershed named Tuogao river watershed, which is located on the north side of Chaohu Basin (31°35'0" N–31°55'0" N, 117°33'0" E–117°57'0" E) is selected as the study area, and Tuogao river watershed is located in Hefei city, Anhui province, China. The total length of Tuogao River is 35 km. The river flows from north to south into Chaohu Lake. In this study, the middle and lower reaches of the Tuogao River (which has an area of 431.2 km²) are selected as the study area. This area is higher

in the north and lower in the south. It is located in a plain polder area, which refers to a plain river network or lakeside and other low-lying waterlogging areas. This area is formed through embankments, sluices, and pumping stations. The purpose of constructing a polder area is to resist floods and waterlogging. The study area is characterized by a north subtropical humid monsoon climate, with annual precipitation of 1000–1158 mm, annual evaporation of 1469–1629 mm, and rainfall concentrated mostly in summer (Cao et al, 2007). At present, the main part of the study area is agricultural land, and the rest consists of grassland, woodland, and residential land .

The study area is listed in figure 1.

(Put figure 1 here)

The study area faces problems of eutrophication and algae growth, and P is a key factor. P comes from NPS pollution caused by local agricultural activities.

The purpose of this study is to reduce the total P release of the study area through BMP spatial optimal allocation. Taking July, when NPS pollution is worst, as an example, this study analyzes the schemes of BMP spatial allocation layout under different reduction targets of P pollution, specifically, 20%, 40%, and 60%.

3. Methodology and material

3.1 Study process

The study process consists of the following steps:

(1) Construction of watershed hydrological model: This task includes collecting basic data on the study area, establishing the basic database of the research area (DEM, soil, and land use), using the SWAT model to divide the study area into sub-basins, and

simulating the P emissions in each sub-basin.

(2) BMP selection and associated uncertainty analysis: This task involves selecting suitable BMP facilities (such as reservoirs, wetlands, and vegetation buffer zones); facility parameters (surface area, facility depth, permeability, and others); and analyzing the uncertainty of BMPS (based on cost uncertainty and P treatment efficacy uncertainty).

(3) Construction of the uncertain fractional optimization model to select the BMP types of each sub-basin and set the number of BMPs, to determine the BMP optimal allocation scheme of the study area, and obtain the optimized P reduction effect and cost.

The flow diagram is list in figure 2.

(Put figure 2 here)

3.2 Construction of watershed hydrology model

3.2.1 Model introduction

SWAT models, which were used many times in related studies, are applied in the study (Ouyang et al., 2012). The SWAT model can divide the studied watershed into a sub-basin and simulate the transformation and migration of P in each sub-basin. In the SWAT model, P input is mainly from inorganic fertilizers and manure used in agricultural activity. The loss of P mainly occurs because of crop absorption, surface runoff, flow measurement, infiltration, and soil erosion (Kaini et al, 2012). The SWAT model can fully consider the changes in regional land use, and soil and agricultural tillage in the simulation of P transformation and migration (Fei et al, 2016).

3.2.2 Database preparation

The SWAT model consists of spatial and meteorological databases. The spatial database includes a digital elevation model (DEM), soil, land use, and others. The elevation data are the 30 m resolution DEM data provided by the international scientific data service platform. The land-use database was derived from the interpretation data of watershed Landsat TM images in 2018. There are 6 types of land use in the river basin in 2018: these are paddy fields, dry fields, woodland, grassland, water bodies, residential areas, and paddy fields in the main area. The soil database uses the soil type (1:11 million) provided by Nanjing soil as input data for the simulation. The Tuogao river basin consists of yellow brown, yellow brown loam, paddy, coarse bone, limestone, and rinsing paddy soil. The main area mainly consists of paddy soil. The meteorological attribute database consists of the data obtained from a local meteorological observatory, including daily water drop, daily maximum/minimum temperature, daily solar radiation, wind speed, and daily average relative humidity.

3.2.3 Parameter validation and calibration

When no observation data are available, the calibration and validation of the parameters could refer to the parameters of other watersheds at the same latitude and natural conditions (Panagopoulos et al., 2011). As there is no long-term effective hydrological observation data in the study area, this study transplanted the parameters of the Xinanjiang River Basin under the same latitude and natural conditions (Wang et al., 2012). At the same time, the previous studies in the case area are considered as a reference (Zheng Zhixia et al., 2011), and the relevant parameters needed for the

simulation of NPS P pollution are finally obtained (Table 1).

Table 1 validated value of SWAT modeling parameters

Parameter	Validated	Parameter	Validated	Parameter	Validated	
CN2.m	FRST	59.54	CANMX.hr	12.616	ALPHA_BF.g	0.1282
	RICE	71.88	ESCO.hru	0.1188	GW_DELAY.g	36.182
	PAST	61.12	GWQMN.g	1274.91	SMTMP.bsn	0.0418
	URM	58.06	Usle.mgt	0.1367	CMN.bsn	0.002
	WAT	85.33	Spexp.bsn	0.76	NPERCO.bsn	0.26
	AGR	73.00	SPCON.bsn	0.0543	PSP.bsn	0.7
PPERCO.bsn	15	CH_K2.rte	38.951	BC2.bsn	2	
BC4.bsn	0.01	TIMP.bsn	0.29	BC3.bsn	0.23	
AI1.wwq	0.08	PHOSKD.b	165	AI2.wwq	0.02	
CH_N2.rte	0.1597	BC1.bsn	0.22	RCDCO.bsn	0.05	

3.2.4 Relevant data of sub-watershed

Through SWAT simulation, the study area is divided into 31 sub-basins. The area of each sub-basin, surface water quantity, and P release amount are shown in Table 2.

Table 2 The area of each sub-basin, surface water quantity, and P release amount in each basin

Serial number	Area (ha)	Volume (m ³)	P emission (kg)
1	2905.30	949596.18	13460.24
2	2735.05	812091.78	11301.24
3	1.15	472.45	4.73
4	372.37	208756.04	1399.38
5	2551.61	863261.32	11665.97
6	234.10	71532.67	1402.94
7	4097.82	1034086.06	17456.73
8	1501.46	429672.59	6184.51
9	64.43	25940.94	427.14
10	3476.11	746042.74	14842.99
11	131.39	49412.60	1044.83
12	1829.82	481754.04	7434.54
13	2754.15	404336.85	6742.16
14	3053.00	730766.05	12886.71
15	652.70	198354.89	3957.96
16	1374.90	448548.42	8901.12
17	1461.62	509054.26	7154.65
18	1465.23	324709.64	6275.58

19	1373.02	443786.87	7658.69
20	1.72	708.07	8.65
21	986.46	162490.48	3440.79
22	1004.91	499378.59	3939.24
23	1735.96	692615.28	10700.49
24	1641.29	657912.61	8895.81
25	500.81	203230.43	3374.49
26	1390.07	555748.78	8261.17
27	1678.92	668359.80	8780.73
28	170.41	69879.21	1317.25
29	36.97	15198.90	270.08
30	1199.74	488726.56	7341.22
31	741.22	299609.15	4965.44

3.3 BMP selection and relevant uncertainty analysis

3.3.1 Analysis of BMP character

Three types of BMPs, which are suitable for the study area, are selected as the study objects. These are:

(1) Vegetation buffer zone

The shore vegetation buffer zone refers to the vegetation zone, which is usually composed of trees and other vegetation that climb to the slopes on both sides of the river bank. The main ways to intercept P in the vegetation filtration zone include plant absorption and soil adsorption (Habibiandehkordi et al, 2020). The way for plants to remove P is root absorption. Sediment removes P by absorbing it, and vegetation filtration zones can intercept P, especially granular P, by intercepting sediment (Sandra et al, 2019, Zhou and Wang, 2014).

(2) Pond system

Reservoirs can remove P from surface runoff produced by rainfall. Reservoirs also

have certain ecological functions. A pond system aims to use a soil microbial plant system to intercept, deposit, absorb, and transform P through physical, chemical, and biological processes to achieve efficient purification of P pollution (Baird et al, 2020). Furthermore, the pond system promotes the growth of green plants and achieves resource utilization and innocuity of P through the biogeochemical cycle of nutrients and water (Li et al, 2018).

(3) Constructed wetlands

Constructed wetlands remove P through the combined action of substrates, aquatic plants, and microorganisms (Jarvie et al, 2020; Dierberg et al, 2020). The substrate is the filler, and its main way to remove P is through adsorption, that is, when runoff flows through the constructed wetland, the substrate purifies and removes P from the runoff through certain physical and chemical pathways such as absorption, adsorption, filtration, ion exchange, and complexation reaction (Fasching et al, 2015). Aquatic plants can transfer inorganic P to organic components of plants through plant absorption and assimilation, and the P absorbed by plants can be removed by regular harvesting. The micro-organisms can transfer the organ P into P phosphate and also increase the solubility of the organic P through the metabolic activity of P bacteria. In this way, the P in the runoff is removed (Widney et al, 2017).

3.3.2 Relevant parameters of BMPs

The volume of NPS treatment of the wetland and pond system depends on its volume and permeability, and the vegetation buffer zone depends on its surface area. In this study, five different scales of BMP facilities were set for the three types of BMPs.

The widths of the coastal vegetation zones are 2,5,10,15, and 20 m.

The depth of the reservoir system is set to 1.6 m. The number of surface areas is set to 5, namely, $0.2\% \cdot A_{sub,i}$, $0.4\% \cdot A_{sub,i}$, $0.6\% \cdot A_{sub,i}$, $0.8\% \cdot A_{sub,i}$, and $1.0\% \cdot A_{sub,i}$, where $A_{sub,i}$ represents the area of the i -th subbasin. The depth of the wetland is set to 0.7 m. The number of surface area types is set to 5, namely, $0.2\% \cdot A_{sub,i}$, $0.4\% \cdot A_{sub,i}$, $0.6\% \cdot A_{sub,i}$, $0.8\% \cdot A_{sub,i}$, and $1.0\% \cdot A_{sub,i}$, where $A_{sub,i}$ represents the area of the i -th subbasin. (Note: The area of the pond system and wetland does not cover only one-unit BMPs, but the total area of the BMPs is no more than the set value.)

Although the capacities of ponds and wetlands are constant values, and the ponds and wetlands involve evaporation and infiltration of water bodies, the formula for calculating the volume of treated water in the ponds and wetlands is as follows: BMP surface area \times (depth of facility + permeability of facility + evaporation).

The water evaporation in July is 0.134 m, the permeability of the reservoir is 3.25 m, and that of wetland is 1.38 m.

The categories of each BMPs are listed in Table 3.

Table 3 The categories of each BMPs

Category	1	2	3	4	5
Vegetataion buffer	2m	5m	10m	15m	20m
Ponds system	$0.2\% \cdot A_{sub,i}$	$0.4\% \cdot A_{sub,i}$	$0.6\% \cdot A_{sub,i}$	$0.8\% \cdot A_{sub,i}$	$1.0\% \cdot A_{sub,i}$
Wetlands	$0.2\% \cdot A_{sub,i}$	$0.4\% \cdot A_{sub,i}$	$0.6\% \cdot A_{sub,i}$	$0.8\% \cdot A_{sub,i}$	$1.0\% \cdot A_{sub,i}$

And the volume of P treatment of the ponds system and the wetlands are calculated as follows

$$Tr_j = ReP_j \cdot EfP_j \quad (1)$$

$$ReP_j = TP_i \cdot ReS_j / TS_i \quad (2)$$

$$\text{ReS}_j = A_j \cdot (\text{DeP}_j + \text{Ev} + \text{In}_j) \quad (3)$$

where

- Tr_j The volume of treated P of j-th BMPs
- ReP_j The volume of retained P of j-th BMPs
- EfP_j The efficiency of P treatment of j-th BMPs
- TP_i Total volume of P emission in i-th sub basin
- ReS_j The retained surface water of j-th BMPs
- TS_i Total volume of surface water in i-th sub basin
- A_j The area of j-th BMPs
- Dep_j The depth of j-th BMPs
- Ev The evaporation rate of the study area in a month
- In_j The infiltration rate of j-th BMPs in a month

3.3.3 P treatment efficiency of BMPs and cost uncertainty analysis

The P treatment process by BMP refers to many factors such as BMP reaction time, temperature, season and plant species, microbial species, and others. Variance in any one of them would cause changes in pollutant removal efficiency. Thus, the removal efficiency of pollutants is the form of interval number. The P process efficiency of BMP is listed in accordance with relevant studies (Nan, 2013; Zhang, 2013). For the economic cost, because the economic cost of BMP is subject to market fluctuations and is also uncertain, the uncertain distribution of cost is listed in accordance with relevant studies (Chang, 2017; Wainger et al, 2011; Yang, 2011). The uncertainty of P treatment efficiency and cost of the three BMPs are listed in table 4.

Table 4. The uncertainty of P treatment efficiency and cost of the three BMPs

	P treatment efficiency	Cost (EUR/ha)
Ponds system	80% ~ 90%	[14.7, 34.3]
Wetlands	25% ~ 90%	[53.9, 80.7]
Vegetation buffer (2m)	30.09% ~ 38.06%	[451.66, 1053.86]
Vegetation buffer (5m)	41.00% ~ 50.92%	[451.66, 1053.86]
Vegetation buffer (10m)	54.22% ~ 65.68%	[451.66, 1053.86]
Vegetation buffer (15m)	69.00% ~ 78.95%	[451.66, 1053.86]
Vegetation buffer (20m)	77.31% ~ 82.96%	[451.66, 1053.86]

And the volume of P which could be processed by BMPs in different grades could be calculated according to the formula and the related parameters. The values are listed in attached tables.

3.4 Construction of optimization model

3.4.1 Model in certain condition

The objective of the model is P treatment maximization and cost minimization. The constraints of the model include total volume of P treatment, allowed area of BMP installation, and number of installed BMPs in each sub-watershed.

Objective function

P treatment maximization:

$$\text{Maximize} = \sum_{i=1}^m \sum_{j=1}^n TP_i \cdot x_{ij} \cdot TrE_{ij} \quad i = 1, 2, \dots, m; \quad j = 1, 2, \dots, n \quad (4)$$

TP_i : The total volume of P emission in the i-th sub basin.

Tr_{ij} : The P treatment efficiency of the j-th BMPs facility in the i-th sub basin.

Cost minimization:

$$\begin{aligned} \text{Maximize} &= \sum_{i=1}^m \sum_{j=1}^n x_{ij} \cdot C_j & i = 1, 2, \dots, m; j \\ &= 1, 2, \dots, n & (5) \end{aligned}$$

C_j : the cost of the j -th BMPs facility.

The two above objective functions include maximum function and minimum function, and the two functions could be integrated by fractional programming. The integrated function is as follows.

$$\begin{aligned} \text{maxf}(x) &= \frac{\sum_{i=1}^m \sum_{j=1}^n TP_i \cdot x_{ij} \cdot \text{TrE}_{ij}}{\sum_{i=1}^m \sum_{j=1}^n x_{ij} \cdot C_j} & i = 1, 2, \dots, m; j \\ &= 1, 2, \dots, n & (6) \end{aligned}$$

Constraint function

The volume of the treated P in the i -th sub basin can not be less than the specific proportion of the total volume of P emission in the same sub basin.

$$\begin{aligned} \sum_{i=1}^m \sum_{j=1}^n TP_i \cdot x_{ij} \cdot \text{TrE}_{ij} &\geq \sum_{j=1}^n TP_i \cdot SP & i = 1, 2, \dots, m; j \\ &= 1, 2, \dots, n & (7) \end{aligned}$$

SP: specific proportion of the total volume of P emission in the i -th sub basin, and the SP in the study are 20%, 40% and 60% respectively.

The volume of the treated P in the i -th sub basin can not be more than the total volume of P emission in the same sub basin.

$$\sum_{i=1}^m \sum_{j=1}^n TP_i \cdot x_{ij} \cdot TrE_{ij} \leq \sum_{j=1}^n TP_i \quad i = 1, 2, \dots, m; j = 1, 2, \dots, n \quad (8)$$

SP: specific proportion of the total volume of P emission in the i-th sub basin.

The allowed area of BMPs installation in the i-th sub basin can not be more than 1% of the area of the same sub basin.

$$\sum_{j=1}^n x_{ij} \cdot A_{ij} \leq 1\% \cdot A_{sub.i} \quad i = 1, 2, \dots, m; j = 1, 2, \dots, n \quad (9)$$

$A_{sub.i}$: the area of the i-th sub basin.

None negative for the variables

$$\sum_{j=1}^n x_{ij} \geq 0 \quad i = 1, 2, \dots, m; j = 1, 2, \dots, n \quad (10)$$

01 setting for BMPs installation

$$x_{ij} = 0|1 \quad i = 1, 2, \dots, m; j = 1, 2, \dots, n \quad (11)$$

3.4.2 Model in uncertain condition

$$\begin{aligned} \max f(x) &= \frac{\sum_{i=1}^m \sum_{j=1}^n TP_i \cdot x_{ij} \cdot TrE_{ij}^{\pm}}{\sum_{i=1}^m \sum_{j=1}^n x_{ij} \cdot C_j^{\pm}} & i = 1, 2, \dots, m; j \\ &= 1, 2, \dots, n & (12) \end{aligned}$$

$$\begin{aligned} \sum_{i=1}^m \sum_{j=1}^n TP_i \cdot x_{ij} \cdot TrE_{ij}^{\pm} &\geq \sum_{j=1}^n TP_i \cdot SP & i = 1, 2, \dots, m; j \\ &= 1, 2, \dots, n & (13) \end{aligned}$$

$$\begin{aligned} \sum_{i=1}^m \sum_{j=1}^n TP_i \cdot x_{ij} \cdot TrE_{ij}^{\pm} &\leq \sum_{j=1}^n TP_i & i = 1, 2, \dots, m; j \\ &= 1, 2, \dots, n & (14) \end{aligned}$$

$$\begin{aligned} \sum_{j=1}^n x_{ij} \cdot A_{ij} &\leq 1\% \cdot A_{sub.i} & i = 1, 2, \dots, m; j \\ &= 1, 2, \dots, n & (15) \end{aligned}$$

$$\begin{aligned} \sum_{j=1}^n x_{ij} &\geq 0 & i = 1, 2, \dots, m; j \\ &= 1, 2, \dots, n & (16) \end{aligned}$$

$$\begin{aligned} x_{ij} &= 0|1 & i = 1, 2, \dots, m; j \\ &= 1, 2, \dots, n & (17) \end{aligned}$$

4. Results and discussion

(1) Through the model that integrates SWAT and interval fractional planning, the BMP spatial optimization layout scheme is obtained. The scheme includes an upper scenario and the scheme of the lower scenario for 20%, 40%, and 60% P reduction targets in July. In each subbasin, the number of set BMPs is only one (the results are shown in Table 5). The total cost and total volume of P under each scenario are shown

in Table 6. Statistics on the number of all BMP facilities under each scenario are shown in Table 7.

Table 5 The spatial optimization layout of BMPs in each scenario

No.	20H	20L	40H	40L	60H	60L
1	Pond 1%	Pond 1%	Buffer 20m	Buffer 20m	Pond 1%	Buffer 15m
2	Pond 1%	Buffer 20m				
3	Buffer 20m	Buffer 20m	Pond 1%	Pond 1%	Pond 1%	Pond 1%
4	Buffer 10m	Buffer 20m	Pond 1%	Buffer 20m	Buffer 20m	Buffer 20m
5	Wet 0.2%	Pond 1%	Pond 1%	Pond 1%	Pond 1%	Buffer 20m
6	Pond 1%	Buffer 20m	Pond 1%	Buffer 20m	Buffer 20m	Buffer 15m
7	Pond 1%					
8	Pond 1%	Pond 1%	Pond 0.8%	Buffer 20m	Pond 1%	Buffer 20m
9	Buffer 20m	Pond 1%	Pond 0.8%	Pond 1%	Buffer 20m	Pond 1%
10	Pond 1%	Pond 1%	Pond 1%	Pond 0.8%	Pond 1%	Pond 1%
11	Buffer 15m	Pond 1%	Pond 1%	Pond 1%	Buffer 20m	Buffer 20m
12	Pond 1%	Pond 1%	Buffer 15m	Pond 1%	Buffer 20m	Pond 1%
13	Pond 1%					
14	Pond 1%	Buffer 20m				
15	Pond 1%					
16	Pond 1%	Buffer 20m				
17	Pond 1%	Pond 1%	Buffer 20m	Pond 0.8%	Buffer 20m	Buffer 20m
18	Pond 1%	Buffer 15m				
19	Pond 1%	Pond 1%	Buffer 20m	Pond 1%	Buffer 20m	Buffer 20m
20	Pond 1%	Buffer 20m				
21	Pond 1%	Buffer 20m				
22	Buffer 20m	Pond 1%				
23	Pond 1%	Pond 1%	Buffer 20m	Buffer 20m	Buffer 20m	Buffer 20m
24	Pond 1%	Pond 1%	Buffer 20m	Buffer 20m	Pond 1%	Buffer 20m
25	Pond 1%	Pond 1%	Pond 1%	Buffer 15m	Buffer 15m	Buffer 15m
26	Pond 1%	Pond 1%	Buffer 20m	Buffer 20m	Buffer 20m	Buffer 20m
27	Pond 1%	Pond 1%	Buffer 15m	Buffer 15m	Buffer 20m	Buffer 20m
28	Buffer 20m	Pond 1%	Buffer 20m	Buffer 20m	Buffer 20m	Buffer 20m
29	Buffer 20m	Buffer 20m	Buffer 20m	Buffer 20m	Pond 1%	Buffer 20m
30	Pond 1%	Buffer 20m	Buffer 15m	Buffer 20m	Buffer 20m	Buffer 20m
31	Buffer 20m	Buffer 20m	Pond 1%	Buffer 20m	Pond 1%	Buffer 20m

Note: The number of BMPs installed in each sub basin is 1 respectively.

where

Pond: Ponds system

Buffer: Vegetation buffer

Wet: Wetland

Table 6 The total cost and the total volume of the treated P

	20%		40%		60%	
	+	-	+	-	+	-
Total cost (EUR)	3990.58	6585.58	5699.22	10955.14	6573.14	17509.48
Total treated P (kg)	38904.15	40483.60	89900.35	80739.23	80622.07	121235.31

Table 7 The number of installed BMPs in each scenario

Type of BMPs		20%		40%		60%	
		+	-	+	-	+	-
wetland	0.20%	1	0	0	0	0	0
	0.40%	0	0	0	0	0	0
	0.60%	0	0	0	0	0	0
	0.80%	0	0	0	0	0	0
	1.00%	0	0	0	0	0	0
Pond	0.20%	0	0	0	0	0	0
	0.40%	0	0	0	0	0	0
	0.60%	0	0	0	0	0	0
	0.80%	0	0	2	3	0	0
	1.00%	22	23	17	14	17	8
Vegetation buffer	2m	0	0	0	0	0	0
	5m	0	0	0	0	0	0
	10m	1	0	0	0	0	0
	15m	1	0	3	2	0	4
	20m	6	8	9	12	14	19
Total number of BMPs		31	31	31	31	31	31

(2) Table 4 shows that under the condition of the same area, whether in the upper or lower limit, according to the P treatment capacity, green buffer zone > reservoir > wetland. Taking the sub basin 1 as an example, we find that Table 8 corresponds to the BMP treatment effect of sub basin 1, and the P control effect of each BMP facility can

be observed. Table 9 shows the ratio of P treatment capacity of the green buffer zone to the wetland and pond system.

Table 8 The BMP treatment effect of sub basin 1

Type of BMPs	Scenario	0.2%	0.4%	0.6%	0.8%	1%
Pond	-	328.14	656.27	984.41	1312.54	1640.68
	+	369.15	738.31	1107.46	1476.61	1845.76
Wetland	-	45.59	91.18	136.76	182.35	227.94
	+	164.12	328.23	492.35	656.47	820.59
Vegetation	-	4038.07	5518.70	7268.53	9287.56	10364.38
	+	5114.89	6864.72	8883.76	10633.59	11172.00

Table 9 The ratio of P treatment capacity of the green buffer zone to the wetland and pond system

Ratio		0.2%	0.4%	0.6%	0.8%	1%
Vegetation buffer/Wetland	-	88.57	60.53	53.15	50.93	45.47
	+	31.17	20.91	18.04	16.20	13.61
Vegetation buffer/Pond	-	12.31	8.41	7.38	7.08	6.32
	+	13.86	9.30	8.02	7.20	6.05

Table 4-5 shows that the P treatment capacity of the green buffer zone is much larger than that of the reservoir and wetland under the same scenario, when the 0.01 scenario is used as an example. In the upper limit scenario, the P treatment capacity of the green buffer zone is 6.05 times that of the pond and 6.32 times in the lower limit scenario. The ratio of the green buffer zone to wetland is 13.61 times in the upper limit and 45.47 times in the lower limit.

(3) In this study, 31 BMPs were assigned under each scenario. However, no upper limit is set for the installed number and the types of BMPs per subbasin in the constraints. The reason is that one-unit BMP is sufficient to cope with the P pollution of the subbasin. Thus, it does not need more than one-unit BMP in a subbasin, and it can be attributed to the strong pollution control ability of the green buffer zone, which

can absorb 77.31%–82.96% of P. The pollution control target, which is under this limit, could be achieved through 20 m of green buffer zones. This study does not limit the budget. In the lower limit scenario of 60% P treatment scenario, the highest budget is 17,509.48 EUR. If the budget is lower than this amount, then it will limit the setting of the high-cost green buffer zone. This condition would also lead to the simulation results in which more ponds and wetlands are installed, and three BMPs are low effective but also low cost of low-effective but also low-cost ponds and wetlands.

(4) According to the results, with the increase of the P pollution reduction target, the number of installed BMPs with higher pollution control effect is increase. In the lower limit scenarios of 20%,40%, and 60% P reduction target, the number of green buffer zones installed are 6, 9, and 14, respectively. In the upper limit scenario, the assigned amounts are 8, 12, and 19. As the total number of BMPs in each scheme is the same, the number of green buffer zones with the highest treatment effect increases, and the number of other types of BMP decreases accordingly.

(5) As the upper limit value of the BMP facility cost and the lower limit value of P pollution control quantity are considered in the lower limit scenario, then on the premise of completing the pollution control target of each grade, the total cost in the upper limit scenario is less than the total cost in the lower limit scenario.

In the 20%, 40%, and 60% scenarios, the total cost of the upper and lower limit scenarios are [6585.58 (lower scenario), 3990.58 (upper scenario)], [10955.14 (lower scenario), 5699.22 (upper scenario)], and [17509.48 (lower scenario), 6573.14 (upper scenario)], respectively.

(6) As the lower limit of the BMP pollution control efficiency is set in the lower limit scenario, and the upper limit is set in the upper limit scenario, the number of green buffer zones with high cost and high pollution control effect in the upper limit scenario under each control target is also smaller than that in the lower limit scenario. This condition means that solving the same volume requires a smaller number of BMP facilities with high P pollution treatment efficiency and high cost.

(7) As the cost and P treatment efficacy in this study are considered as the upper and lower limit values, the uncertain values of the cost and treatment efficiency of BMPs are also expressed as interval numbers. Thus, the results are in the form of the upper and lower limit scenarios. The results represent the upper and lower limits of the corresponding schemes under uncertainty impact, which means that the schemes are reasonable when their results are in the interval range.

5. Conclusion

(1) The innovation of this study is that it designs a model that integrates SWAT and interval fractional programming to optimize the BMP spatial optimization layout in watersheds under uncertainty. The model can effectively reflect and deal with the uncertainty in P pollution treatment efficiency and cost of BMPs. Thus far, the method has not been applied to studies on BMP spatial optimization layout.

(2) According to the spatial layout scheme corresponding to the upper and lower limit scenarios under different P pollution reduction targets, the upper and lower limit scenarios represent the limit of uncertainty impact on the scheme. The scheme is

reasonable when it is in the interval. The total costs in the research results are also interval numbers, and the total cost in practical terms is also in the interval.

(3) The developed method provides the schemes that correspond to the upper and lower limit scenarios. The method can provide more reasonable schemes for decision-makers under uncertain conditions.

(4) Different from the genetic algorithm method usually used in BMPs spatial optimization layout, this study does not need to set all variables as uncertainty number, nor does it need to set the average value for uncertainty numbers. Because it is always difficult to identify the uncertainty distribution mode in practice. Therefore, the developed method in this study can be better used in practical condition.

Declaration

Ethical Approval

Not applicable. There is no human experiment or animal experiment in the study, and the study does not address the ethical issue.

Consent to Participate

Not applicable.

Consent to Publish

Not applicable.

Authors Contributions

Jinjin Gu developed the model and calculated the data.

Yuan Cao analyzed the uncertainty of the related data and draw the figure.

Min Wu, Min Song and Lin Wang help collect the data and helped develop the model and also helped examine the manuscript.

All authors read and approved the final manuscript.

Funding

We gratefully acknowledge financial supports for this research from projects of National Natural Science Foundation of China (Grant No. 41601581); Fundamental Research Funds for the Central Universities (Grant No. JZ2019HGBZ0163); Philosophy and Social Science Cultivation Program of Hefei University of Technology (Grant No. JS2020HGXJ0021).

Competing Interests

The authors declare that there are no conflicts of interest regarding the publication of this paper.

Availability of data and materials

All data generated or analyzed during this study are included in the manuscript and attached table.

References

Baird J.B., Winston R.J., Hunt W.F. (2020), Evaluating the hydrologic and water quality performance of novel infiltrating wet retention ponds. *Blue-Green Systems*, 2(1):282-299.

Cao Q, Tao W.Y., Ma Z.Y., et al (2007), Study on features of chaohu lake basin's evaporation and trend of its variation. *Resource Development and Market*, 23(9): 811-

814.

Chang J. (2017), The applied research of best management practices based on SWAT model[D]. Zhejiang University. (In Chinese)

Dierberg FE, Debusk TA, MD Kharbanda, et al (2020), Long-term sustainable phosphorus (P) retention in a low-P stormwater wetland for Everglades restoration[J]. *Science of The Total Environment*, 756:143386.

Fasching S., Norland J., Desutter T., et al (2015), The Use of Sediment Removal to Reduce Phosphorus Levels in Wetland Soils. *Ecological Restoration*, 33(2):131-134.

Fei X., Dong G., Wang Q., et al (2016), Impacts of DEM uncertainties on critical source areas identification for non-point source pollution control based on SWAT model. *Journal of Hydrology*, 540:355-367.

Feng M., Shen Z. (2021), Assessment of the Impacts of Land Use Change on Non-Point Source Loading under Future Climate Scenarios Using the SWAT Model. *Water*, 13(6):874.

Getahun E., Keefer L., et al (2016), Integrated modeling system for evaluating water quality benefits of agricultural watershed management practices: Case study in the Midwest. *Sustainability of Water Quality and Ecology*, 8:14-29.

Gu J.J., Hu H., Wang L., et al (2020), Fractional Stochastic Interval Programming for Optimal Low Impact Development Facility Category Selection under Uncertainty. *Water Resources Management*, 34:1567 - 1587.

Gu J.J., Zhang Q., Gu D.Z., et al (2018), The Impact of Uncertainty Factors on Optimal Sizing and Costs of Low-Impact Development: a Case Study from Beijing,

China. *Water Resources Management*, 32: 4217-4238

Gu J.J., Zhang X., Xuan X., et al (2020), Land use structure optimization based on uncertainty fractional joint probabilistic chance constraint programming. *Stochastic Environmental Research and Risk Assessment*, 34(11):1699-1712.

Guo P., Chen X., Mo L., et al (2014), Fuzzy chance-constrained linear fractional programming approach for optimal water allocation. *Stochastic Environmental Research & Risk Assessment*, 28(6):1601-1612.

Habibiandehkordi R., Lobb D.A., Sheppard S.C., et al (2020), Uncertainties in vegetated buffer strip function in controlling phosphorus export from agricultural land in the Canadian prairies. *Environmental Science and Pollution Research*, 24(2):1-11.

Jarvie H.P., Pallett D.W., Schfer S.M., et al (2020), Biogeochemical and climate drivers of wetland phosphorus and nitrogen release: Implications for nutrient legacies and eutrophication risk. *Journal of Environmental Quality*, 49(6).

Kaini P., Artita K., Nicklow J.W. (2012), Optimizing Structural Best Management Practices Using SWAT and Genetic Algorithm to Improve Water Quality Goals. *Water Resources Management*, 26(7):1827-1845.

Li M., Li J., Singh V.P., et al (2019), Efficient allocation of agricultural land and water resources for soil environment protection using a mixed optimization-simulation approach under uncertainty. *Geoderma*, 353:55-69.

Li Y.F., Liu H.Y., Liu Z.J, Lou C.Y., Wang J. (2018), Effect of different multi-pond network landscape structures on nitrogen retention over agricultural watersheds. 39(11): 161-168. (In Chinese)

Nan Z. (2013), The study of the risk assessment of NPS pollution and BMPs category selection in Beijing small watershed[D]. Capital Normal University. (In Chinese)

Panagopoulos Y., Makropoulos C., Baltas E., et al (2011), SWAT parameterization for the identification of critical diffuse pollution source areas under data limitations. *Ecological Modelling*, 222(19):3500-3512.

Ouyang W., Huang H.B., Cai G.Q. (2014), Temporal and spatial characteristics of diffuse phosphorus pollution in the watershed without monitoring data at Chaohu Lake. *Acta Scientiae Circumstantiae*, 34(4) : 1024-1031. (In Chinese)

Qi Z., Kang G., Wu X., et al (2020), Multi-Objective Optimization for Selecting and Siting the Cost-Effective BMPs by Coupling Revised GWLF Model and NSGAI Algorithm. *Water*, 12(1):235.

Qiu J., Shen Z., Chen L., et al (2019), Quantifying effects of conservation practices on non-point source pollution in the Miyun Reservoir Watershed, China. *Environmental Monitoring and Assessment*, 191(9):582.1-582.21.

Sandra, Hille, Daniel, et al (2019), Management Options to Reduce Phosphorus Leaching from Vegetated Buffer Strips. *Journal of Environmental Quality*, 48(2):322-329

Wang X., Wang Q., Wu C., et al (2012), A method coupled with remote sensing data to evaluate non-point source pollution in the Xin'anjiang catchment of China. *Science of the Total Environment*, 430: 132-143.

Widney S., Klein A.K., Ehman J., et al (2017), The value of wetlands for water

quality improvement: an example from the St. Johns River watershed, Florida. *Wetlands Ecology & Management*. 26: 265 - 276.

Zheng Z.X., Song malin (2011), Modeling Research on Transfer Processes of Nitrogen and Phosphorus in Different Farmlands from Zhegao River Watershed. *Journal of Anhui Agricultural Sciences*, 39(013):7667-7669. (In Chinese)

Zhou S.S., Wang D.M. (2014), The review on purification mechanism and its influencing factors of riparian buffers. 12(5):114-120. (In Chinese)

Wainger L., Wolcott R., Almeter A., et al (2011), An optimization approach to evaluate the role of ecosystem services in Chesapeake Bay restoration strategies.

Wu H., Zhu A.X., Liu J., et al (2018), Best Management Practices Optimization at Watershed Scale: Incorporating Spatial Topology among Fields. *Water Resources Management*, 32: 155–177

Wu J.H., Lu J. (2019), Landscape patterns regulate non-point source nutrient pollution in an agricultural watershed. *Science of The Total Environment*, 669:377-388.

Yang Y.H., Yan B.X. (2011), Optimal Non-Point Source Pollution Control Practices for a Small Watershed. *Journal of Ecology and Rural Environment*. 27(2): 11-15. (In Chinese)

Zhang G.F. (2013), The Effects of Riparian Vegetation Buffer Zones on Nitrogen and Phosphorus Reduction in Chaobai River Upstream. *Chinese Agricultural Science Bulletin*, 29(8): 189-194. (In Chinese)

Zhang Y.F., Li Y.P., Sun J., et al (2019), Optimizing water resources allocation and soil salinity control for supporting agricultural and environmental sustainable

development in Central Asia. Science of The Total Environment, 704:135281.

Figures

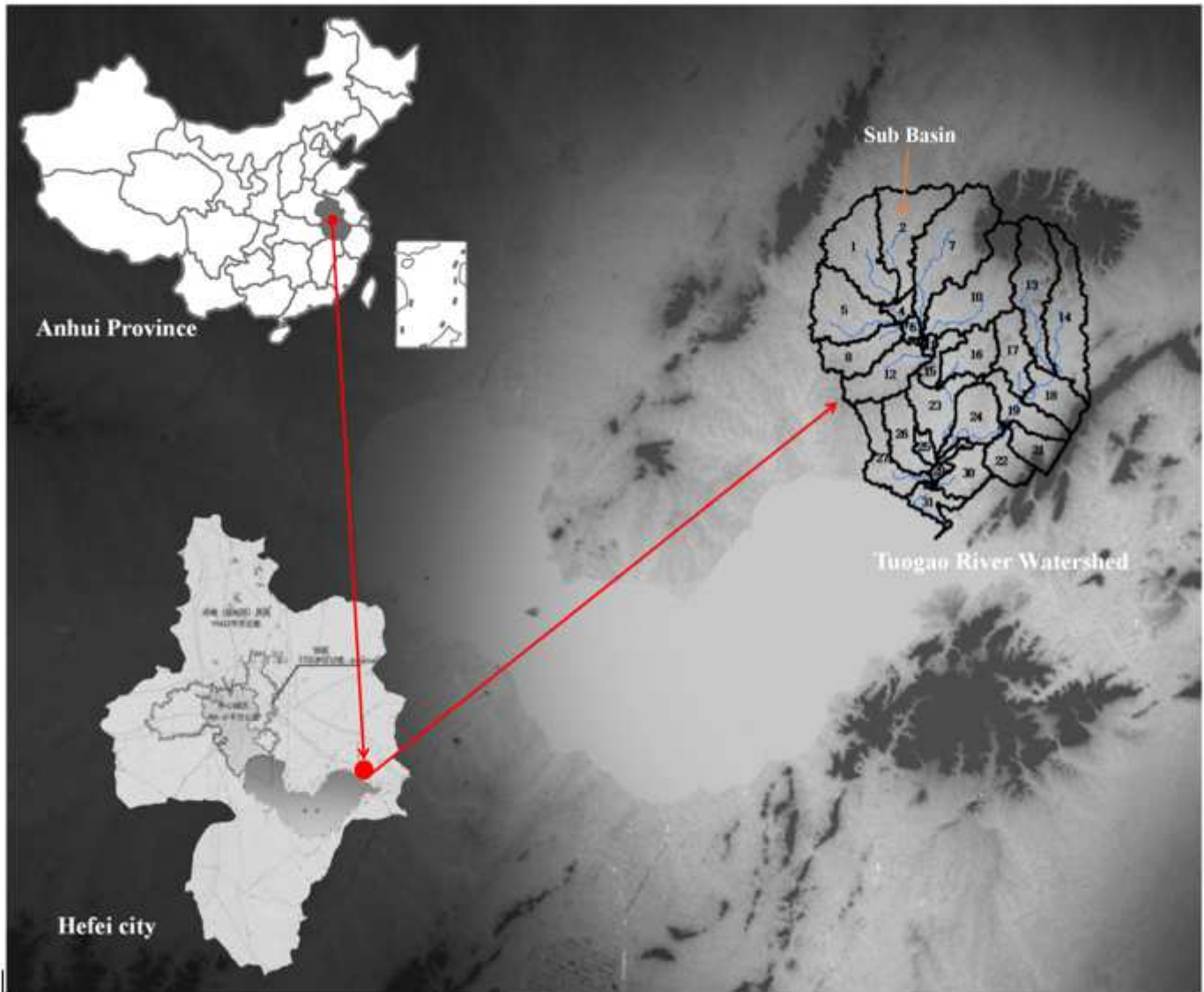


Figure 1

The study area Note: The designations employed and the presentation of the material on this map do not imply the expression of any opinion whatsoever on the part of Research Square concerning the legal status of any country, territory, city or area or of its authorities, or concerning the delimitation of its frontiers or boundaries. This map has been provided by the authors.

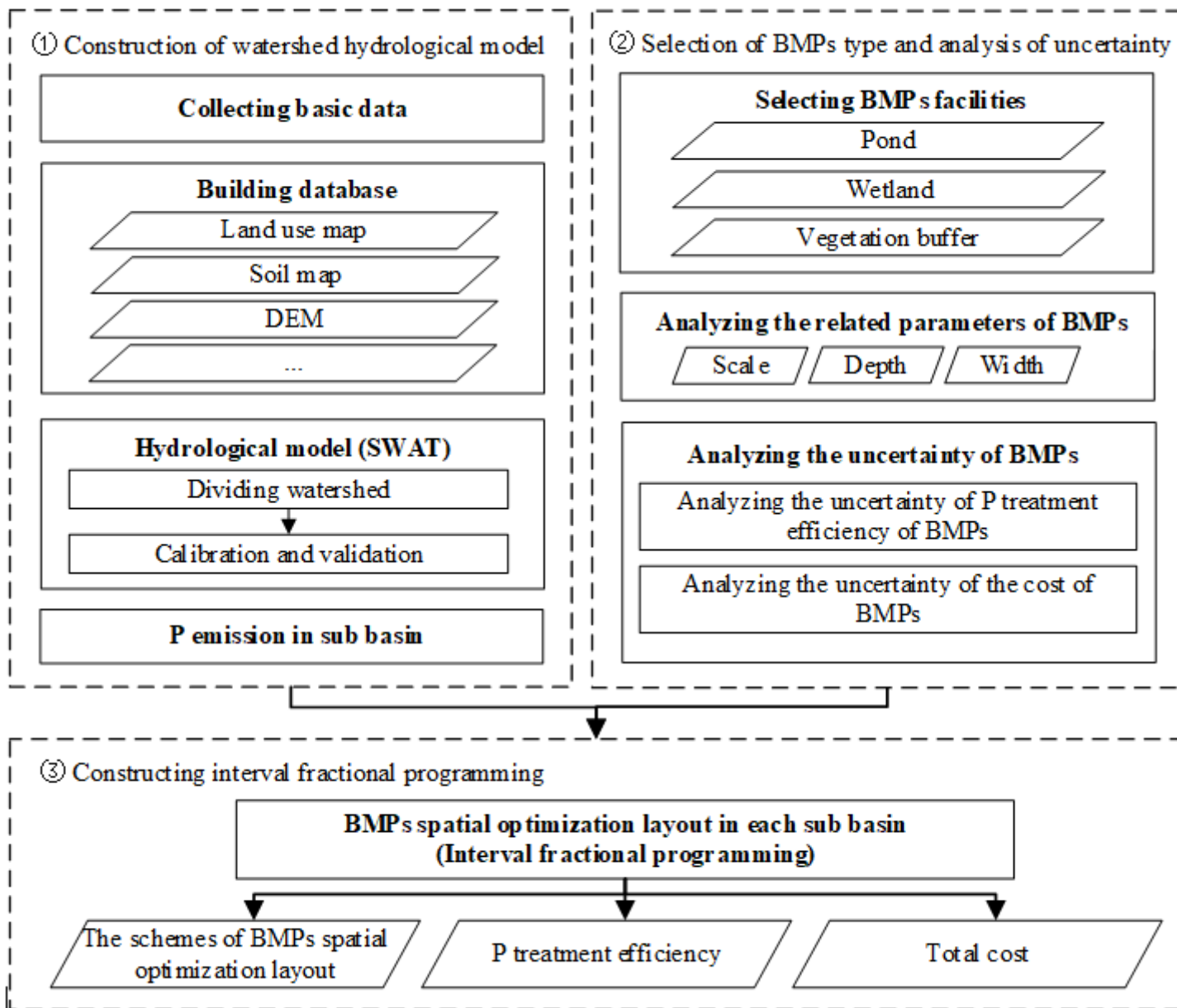


Figure 2

The flow diagram

Supplementary Files

This is a list of supplementary files associated with this preprint. Click to download.

- [attachedtable.docx](#)